Int. J. Electrochem. Sci., 7 **(2012)** 12110 - 12120

International Journal of
ELECTROCHEMICAL
SCIENCE
www.electrochemsci.org

Electrochemical and Physical Properties of Layered-Spinel Composite Cathode Powders Prepared by Spray Pyrolysis

Chul Min Sim[1], *Young Jun Hong*[1], *Min Ho Kim*[1], *Yong Seung Jang*[1], *Byung Kyu Park*[2], *Yun Chan Kang*[1,*]

[1]Department of Chemical Engineering, Konkuk University, 1 Hwayang-dong, Gwangjin-gu, Seoul 143-701, Korea
[2]Suncheon Center, Korean Basic Science Institute, Suncheon 540-742, Korea
*E-mail: yckang@konkuk.ac.kr

Received: 6 October 2012 / *Accepted:* 23 October 2012 / *Published:* 1 December 2012

The $x$$Li_2MnO_3$·(1-$x$)$Li_4Mn_5O_{12}$ (x = 1, 0.5, 0.3, 0) composite cathode powders are prepared by spray pyrolysis. The composite powders before and after post-treatment at 600°C have fine size and aggregated spherical morphologies of the nanometer-sized primary particles irrespective of the compositions of the cathode powders. The initial discharge capacity of the Li_2MnO_3 component is 258 mAh g^{-1}, in which the Coulombic efficiency is 85%. The discharge capacity of the Li_2MnO_3 powders drops from 258 to 115 after 10 cycles. The initial discharge capacities of $x$$Li_2MnO_3$·(1-$x$)$Li_4Mn_5O_{12}$ composite powders are 225 ,219 and 211 mAh g^{-1} when the x values are 0.5 ,0.3 and 0. The capacity retentions of the composite powders are 88, 90, and 83 % after 30 cycles when the x values are 0.5, 0.3, and 0.

Keywords: composite material; cathode material; spray pyrolysis; lithium battery

1. INTRODUCTION

The spinel materials have been investigated as promising class of cathode materials because of their excellent rate capability, low cost, abundance, high safety, easily preparing and nontoxicity [1-9]. However, its application has been limited because of capacity fading at elevated temperatures and an innate low capacity at 4V [10]. Johnson et al. [11] introduced Li_2MnO_3-$Li_{1+y}Mn_{2-y}O_4$ spinel composite material, and it showed a high rechargeable capacity >250 mAh g^{-1} when cycled between 2 and 5 V. The effect of composition of the layered-spinel composite cathode powders prepared by solid state reaction method on the electrochemical properties was mainly investigated.

The electrochemical properties of the composite cathode powders were strongly affected by the compositions of the cathode as well as the physical properties of the powders, such as mean size,

surface area, morphology, and crystallinity [12-15]. The preparation process of the composite cathode powders affects the physical properties of the powders [16-22]. In addition, the physical properties of the powders were affected by the composition of the composite cathode materials even at the same preparation process. Therefore, the effect of composition on physical and electrochemical properties of the composite cathode powders should be investigated in the same preparation process.

Spray pyrolysis, a gas-phase reaction method, was profitable for the preparation of spinel $LiMn_2O_4$ cathode powders [23-25]. Although spray pyrolysis is easy to control the composition of the cathode materials and synthesize highly pure, fine-sized and spherical cathode powders [26-32], it has not been applied to the preparation of Li-rich spinel cathode powders. In this study, the $x Li_2MnO_3 \cdot (1-x) Li_4Mn_5O_{12}$ (x = 1, 0.5, 0.3, 0) composite cathode powders were prepared by spray pyrolysis. The effects of the ratio of Li_2MnO_3 and $Li_4Mn_5O_{12}$ phases on the physical and electrochemical properties of the composite cathode powders were investigated.

2. EXPERIMENTAL

The spray pyrolysis process consisted of three parts; a six-pack ultrasonic spray generator operated at 1.7 MHz, a 1000-mm-long tubular quartz reactor of 50-mm ID, and a bag filter for collecting particles. The precursor solution was prepared by dissolving a stoichiometric amount of lithium nitrate (98%, Junsei) and manganese nitrate hexahydrate (97%, Junsei) in distilled water. The overall concentration of the Li and Mn components in the solution was 0.5 M. The powders were obtained by spray pyrolysis at 900◦C. The flow rate of air used as the carrier gas was fixed at 20 L min^{-1}. The precursor powders obtained by spray pyrolysis were post-treated in a box furnace at 600◦C.

The crystal structures of the prepared cathode powders were investigated using X-ray diffractometry (XRD; RIGAKU DMAX-33) with Cu Kα radiation (λ = 1.5418 Å) at the Korea Basic Science Institute (Daegu). The morphological characteristics of the powders were investigated using scanning electron microscopy (SEM; JEOL, JSM-6060). The cathode electrode was prepared from a mixture containing 20 mg of $x Li_2MnO_3 \cdot (1-x) Li_4Mn_5O_{12}$ and 12 mg of TAB (TAB is a mixture of 9.6 mg of teflonized acetylene black and 2.4 mg of a binder). Lithium metal and a polypropylene film were used as the counter electrode and the separator, respectively. The electrolyte was 1 M $LiPF_6$ in a 1:1 mixture by volume of ethylene carbonate (EC)/dimethyl carbonate (DMC). The cell was assembled in a glove box in an argon atmosphere.

3. RESULT AND DISCUSSION

The morphologies of the precursor powders obtained by spray pyrolysis according to the ratio of Li_2MnO_3 and $Li_4Mn_5O_{12}$ are shown in Fig. 1. The precursor powders had aggregated spherical morphologies of the nanometer-sized primary particles irrespective of the compositions of the cathode powders. The precursor powders prepared directly by spray pyrolysis had poor electrochemical properties because of low crystallinity and phase inhomogeneity. Therefore, the precursor powders

were post-treated at various temperatures to improve the electrochemical properties of the cathode powders. The optimum post-treatment temperature of the composite cathode powders showing the good electrochemical properties was 600°C. Fig. 2 shows the SEM images of the $x$$Li_2MnO_3$·(1-$x$)$Li_4Mn_5O_{12}$ powders post-treated at 600°C. The morphologies of post-treated cathode powders were similar to those of the precursor powders in Figs. 1 and 2.

The XRD patterns of the xLi_2MnO_3·(1-x)$Li_4Mn_5O_{12}$ (x = 1, 0.5, 0.3, 0) powders post-treated at 600°C are shown in Fig. 3. The pure Li_2MnO_3 have a monoclinic structure with a space group of $C2/m$, which structure is the same as that of $R3m$ layered rock-salt structures [33]. The clear splitting of (135) and (060) peaks located at 2θ = 64.5◦ and 65.5◦, which indicates the degree of development of the monoclinic structure of Li_2MnO_3, was shown in the pure Li_2MnO_3 [33]. The pure $Li_4Mn_5O_{12}$ powders had small impurity peaks of monoclinic Li_2MnO_3 at 2θ = 21◦ and 65.5◦ as shown by arrows in Fig. 3(d).

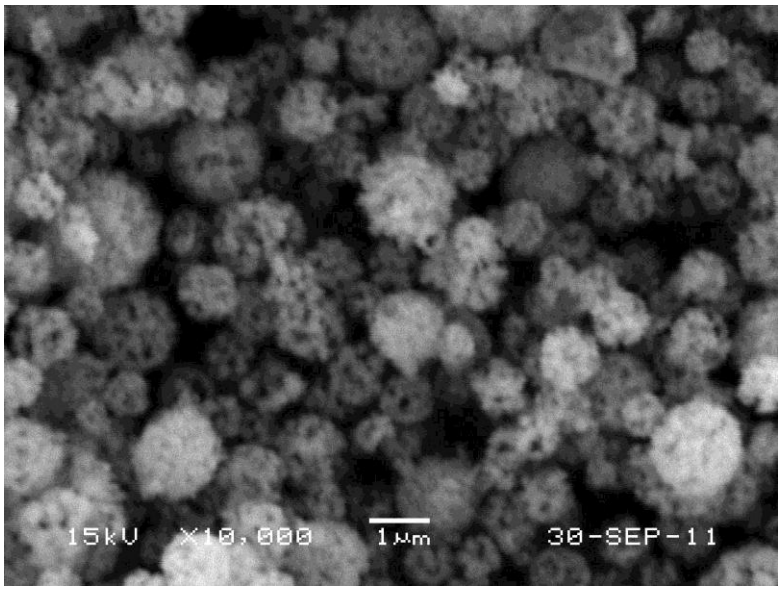

(a)

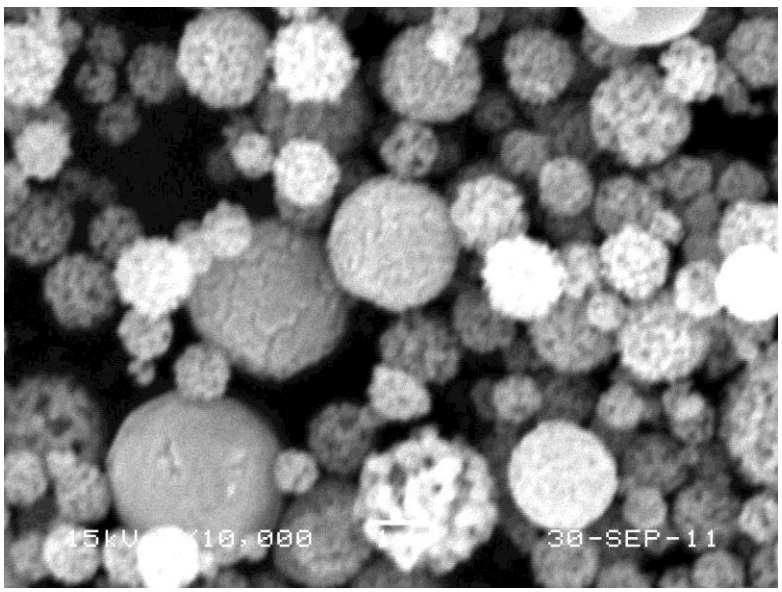

(b)

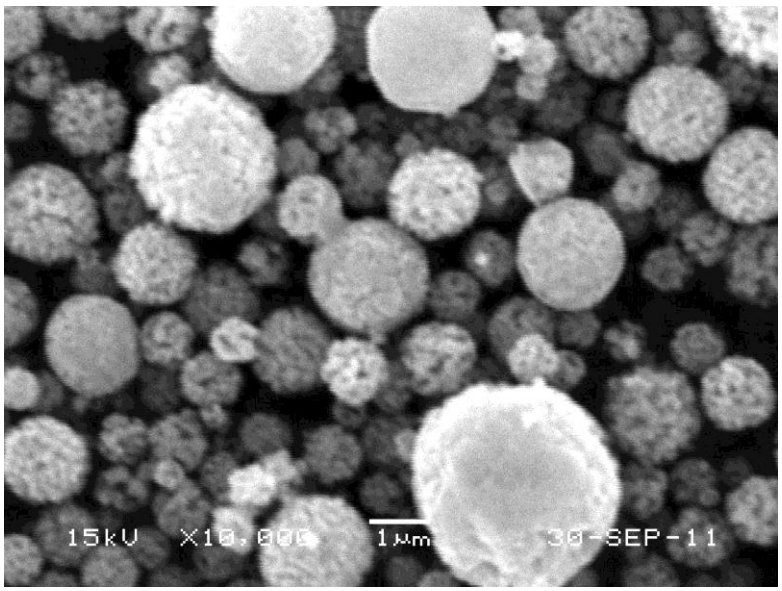

(c)

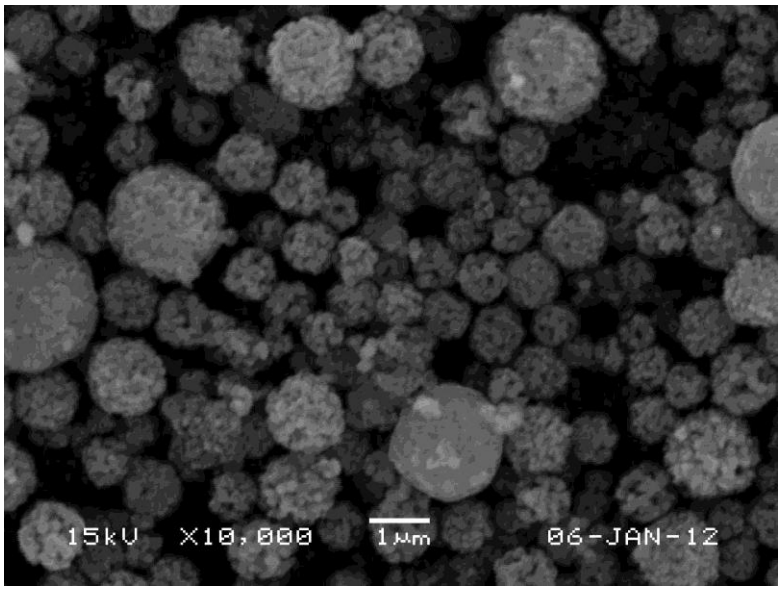

(d)

Figure 1. SEM images of the precursor powders prepared by spray pyrolysis: (a) Li_2MnO_3; (b) $0.5Li_2MnO_3$-$0.5Li_4Mn_5O_{12}$; (c) $0.3Li_2MnO_3$-$0.7Li_4Mn_5O_{12}$; (d) $Li_4Mn_5O_{12}$.

Slight decomposition of the spinel $Li_4Mn_5O_{12}$ phase formed the impurity phase of Li_2MnO_3. The peak intensity of the monoclinic Li_2MnO_3 at 2θ = 21◦ and 65.5◦ increased when the x value increased from 0 to 1. According to increasing the amount of Li_2MnO_3 component, XRD patterns shifted to lower angles.

Fig. 4 shows the initial charge-discharge curves of $xLi_2MnO_3 \cdot (1\text{-}x)Li_4Mn_5O_{12}$ powders post-treated at 600^{o}C at a constant current density of 23 mA g^{-1} between 2.0 and 4.95 V at room temperature. The initial charge and discharge capacities of $xLi_2MnO_3 \cdot (1\text{-}x)Li_4Mn_5O_{12}$ powders increased with increasing the amount of Li_2MnO_3 component. The initial charge and discharge capacities of pure Li_2MnO_3 powders were 302 and 258 mAh g^{-1}, respectively. However, the values of

the pure $Li_4Mn_5O_{12}$ powders were 68 and 211 mAh g^{-1}, respectively. The Li_2MnO_3 component commonly shows no electrochemical reaction at low operating voltages [33]. However, the pure Li_2MnO_3 powders prepared by spray pyrolysis show high initial charge/discharge capacities in the first cycle. The prepared Li_2MnO_3 powders were activated and the two lithium ions were removed from Li_2MnO_3 with concomitant loss of oxygen resulting in the formation of Li_2O and MnO_2 at a high voltage, above 4.6 V, in the initial charge process [11,34]. The initial charge and discharge curves of the pure $Li_4Mn_5O_{12}$ and $xLi_2MnO_3 \cdot (1-x)Li_4Mn_5O_{12}$ composite powders showed the characteristics of the layered and spinel composite powders irrespective of the composition. The initial charge capacities of the composite powders increased from 68 to 116 mAh g^{-1} when the *x* value increased from 0 to 0.5.

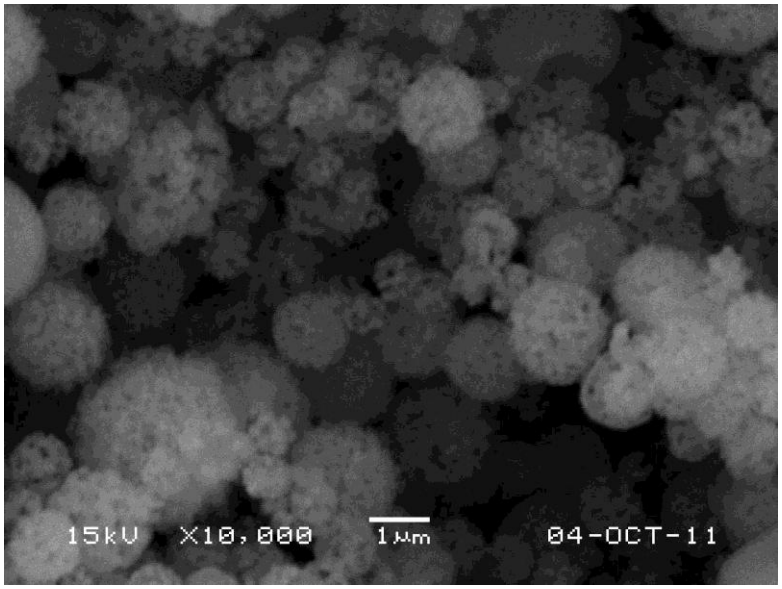

(a)

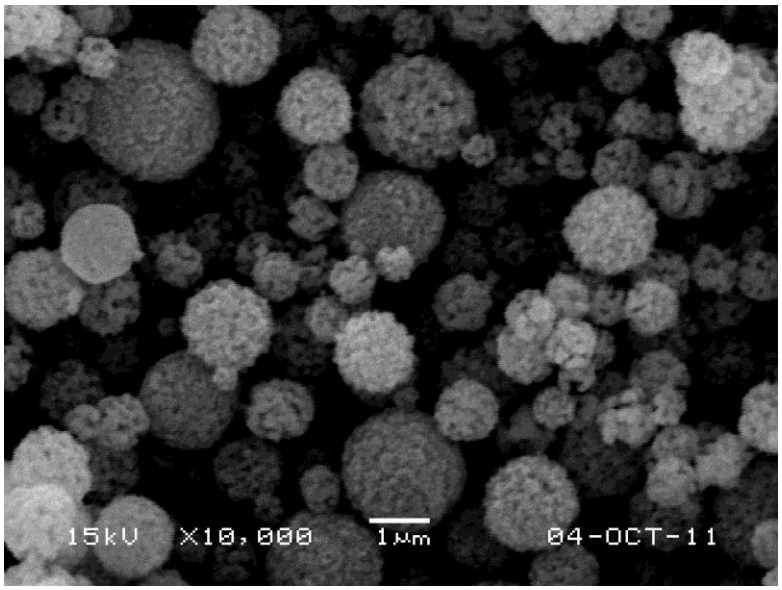

(b)

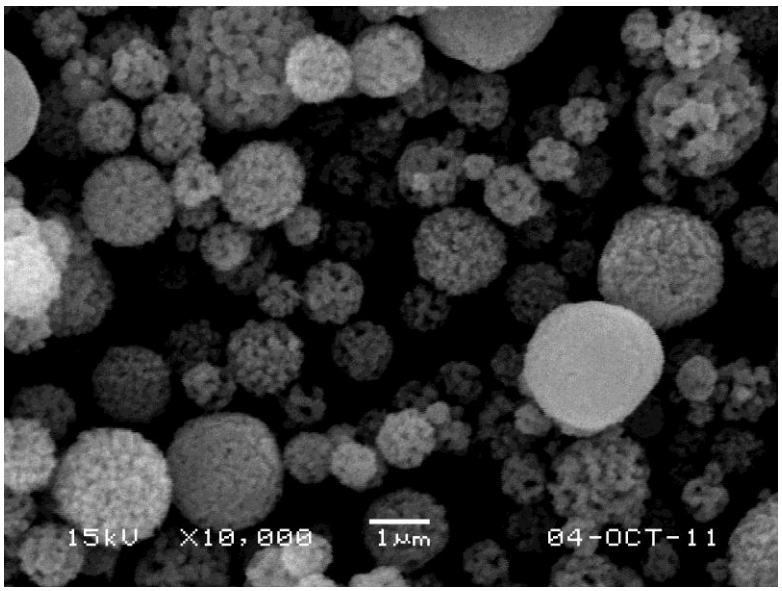

(c)

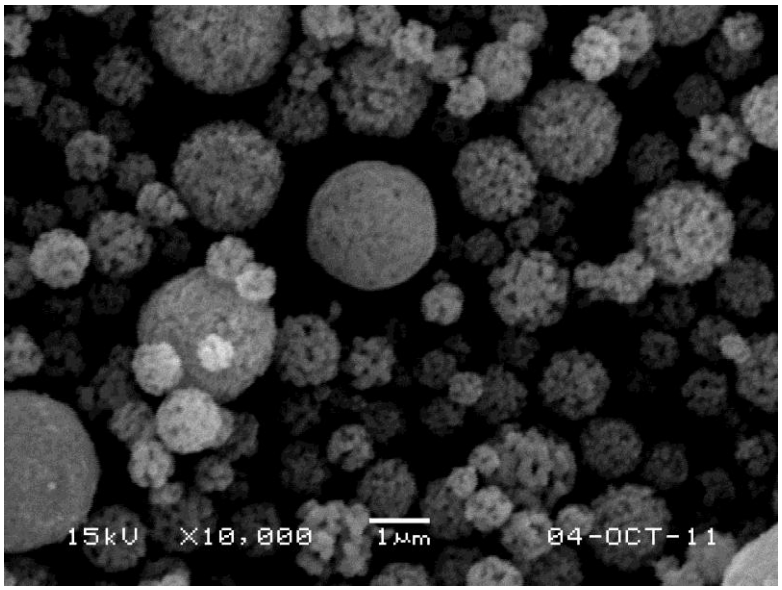

(d)

Figure 2. SEM images of the $x$$Li_2MnO_3$·(1-$x$)$Li_4Mn_5O_{12}$ powders post-treated at 600^{o}C: (a) Li_2MnO_3; (b) 0.5Li_2MnO_3-0.5$Li_4Mn_5O_{12}$; (c) 0.3Li_2MnO_3-0.7$Li_4Mn_5O_{12}$; (d) $Li_4Mn_5O_{12}$.

The composite powders had similar charge capacities due to the $Mn^{3+/4+}$ redox reaction of the spinel component when they were initially charged to 4.5 V (about 35 mAh g^{-1}). The small charge capacities of the powders below 4.5 V indicate that a small amount of Mn^{3+} exists in the pure $Li_4Mn_5O_{12}$ and Li_2MnO_3·$Li_4Mn_5O_{12}$ composite powders [35]. The voltage plateaus in the initial charge curves near 4.75 V were attributed to the removal of Li_2O from the layered Li_2MnO_3 component [11,34]. The initial discharge capacity of the Li_2MnO_3 component was 258 mAh g^{-1}, in which the Coulombic efficiency was 85%. The pure Li_2MnO_3 had a low theoretical Coulombic efficiency [36]. However, the Li_2MnO_3 powders obtained by spray pyrolysis after post-treatment at 600^{o}C had high Coulombic efficiency of 85% because some amount of Mn^{3+} exists in the powders. The charge

capacity below 4.5 V due to the $Mn^{3+/4+}$ redox reaction of the Li_2MnO_3 component was shown in Fig. 4 (a). The Li_2MnO_3 component prepared by spray pyrolysis also had a layered-spinel composite structure. The initial discharge capacities of the $xLi_2MnO_3 \cdot (1\text{-}x)Li_4Mn_5O_{12}$ composite powders slightly increased from 211 to 225 mAh g^{-1} when the *x* value increased from 0 to 0.5. The composite powders had high initial discharge capacities irrespective of the compositions.

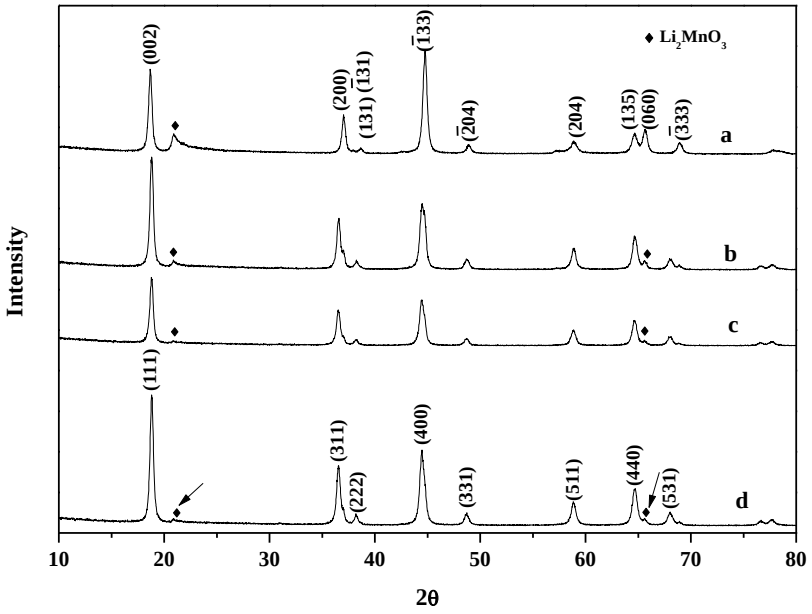

Figure 3. XRD patterns of the powders post-treated at 600°C: (a) Li_2MnO_3; (b) $0.5Li_2MnO_3$-$0.5Li_4Mn_5O_{12}$; (c) $0.3Li_2MnO_3$-$0.7Li_4Mn_5O_{12}$; (d) $Li_4Mn_5O_{12}$.

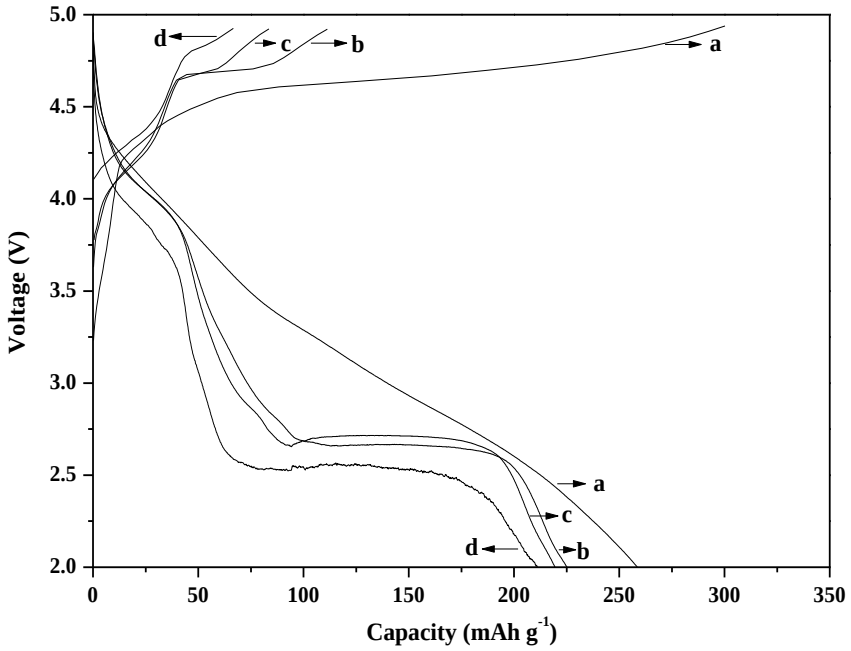

Figure 4. First charge-discharge curves of the powders: (a) Li_2MnO_3; (b) $0.5Li_2MnO_3$-$0.5Li_4Mn_5O_{12}$; (c) $0.3Li_2MnO_3$-$0.7Li_4Mn_5O_{12}$; (d) $Li_4Mn_5O_{12}$.

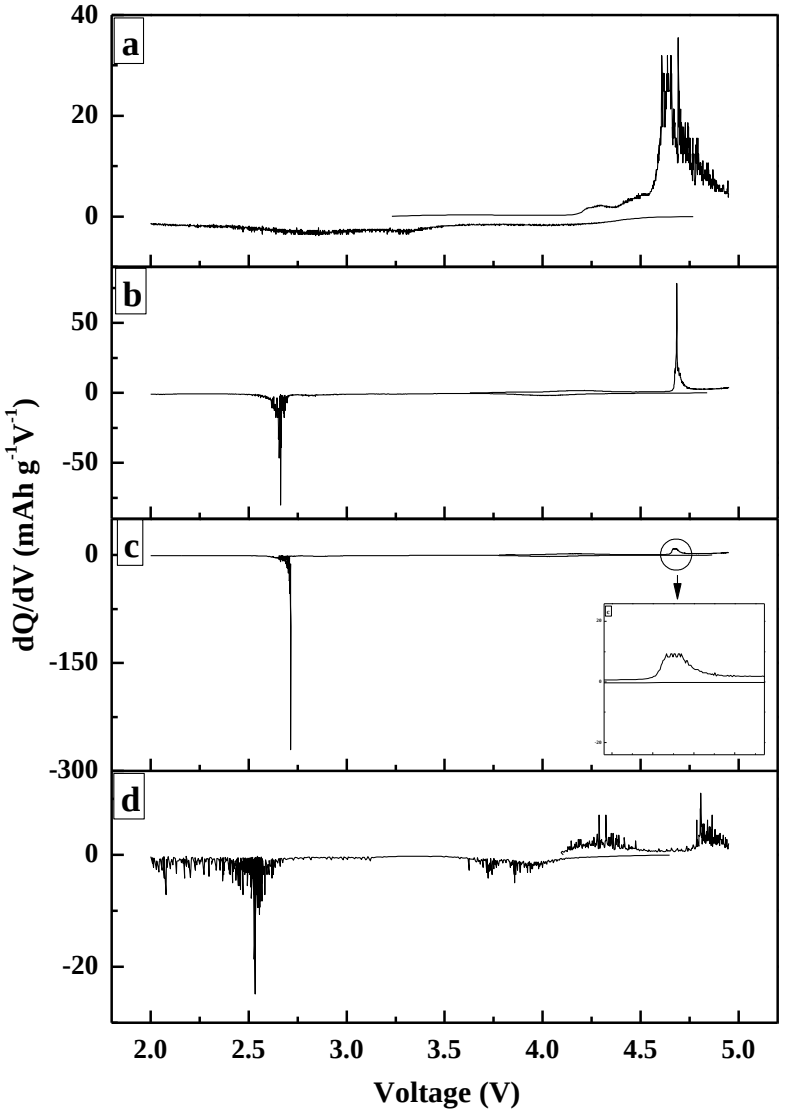

Figure 5. *dQ/dV* curves of the initial cycles of the powders: (a) Li_2MnO_3; (b) $0.5Li_2MnO_3$-$0.5Li_4Mn_5O_{12}$; (c) $0.3Li_2MnO_3$-$0.7Li_4Mn_5O_{12}$; (d) $Li_4Mn_5O_{12}$ post-treated at 600°C.

The initial charge/discharge profiles of the prepared composite powders were similar to those of the $Li_4Mn_5O_{12}$ powders prepared by solid state reaction at 400°C [11]. The lithium extraction and insertion mechanism in $Li_4Mn_5O_{12}$ powders was described in the previous literature [37]. Fig. 5 shows the differential capacity versus voltage (*dQ/dV*) curves of the first cycles as shown in Fig. 4. $xLi_2MnO_3 \cdot (1\text{-}x)Li_4Mn_5O_{12}$ powders had oxidation peaks at around 4.7 V, and the peak intensities increased with increasing the *x* values. It means that the removal of Li_2O from Li_2MnO_3 phase to form the MnO_2 component increased with increasing the *x* values. The cathode powders had reduction peaks below 3.5 V, which can be assigned to the redox-reaction of Mn^{4+}/Mn^{3+} of spinel component, in the initial discharge curves irrespective of *x* values [38].

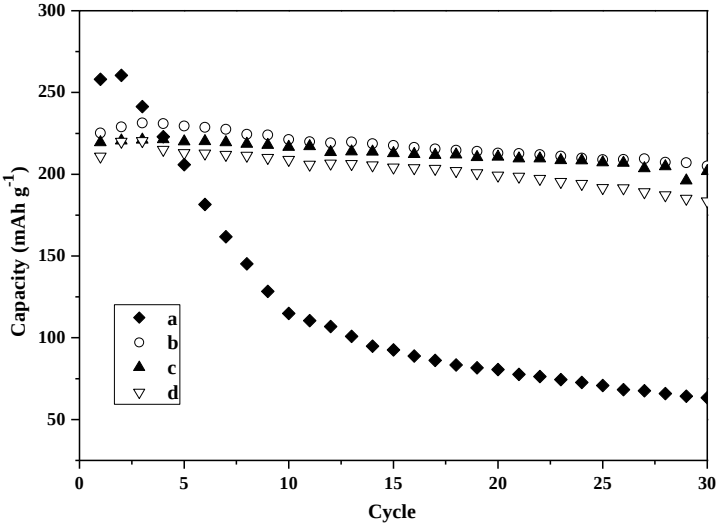

Figure 6. Cycling performance of the powders: (a) Li_2MnO_3; (b) $0.5Li_2MnO_3$-$0.5Li_4Mn_5O_{12}$; (c) $0.3Li_2MnO_3$-$0.7Li_4Mn_5O_{12}$; (d) $Li_4Mn_5O_{12}$.

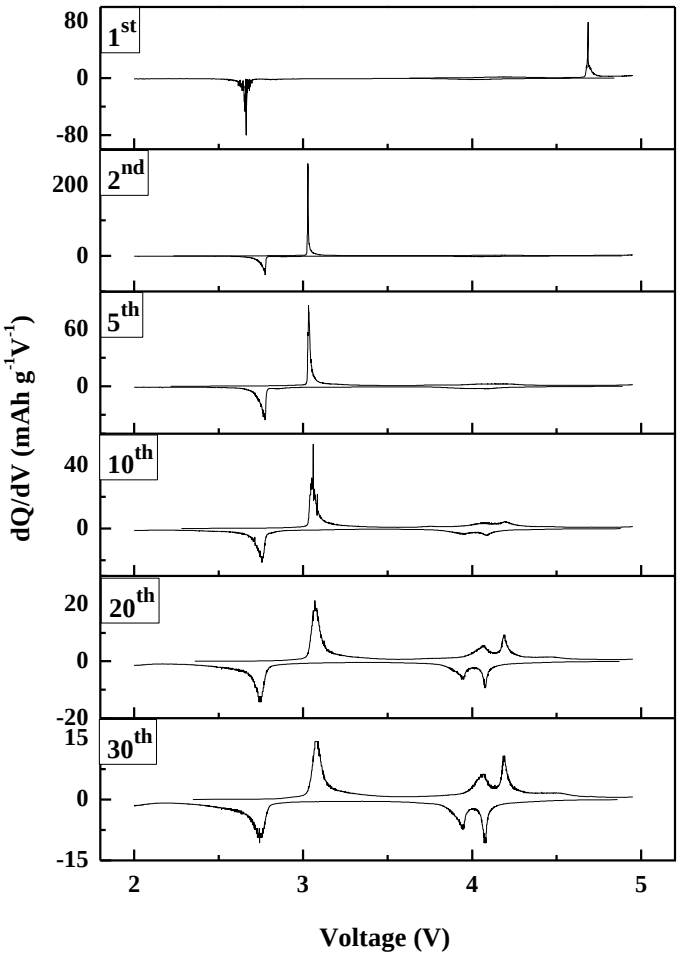

Figure 7. *dQ/dV* curves according to the cycles of $0.5Li_2MnO_3$-$0.5Li_4Mn_5O_{12}$ powders post-treated at 600°C.

Fig. 6 shows the cycle performances of $x\mathrm{Li_2MnO_3}\cdot(1\text{-}x)\mathrm{Li_4Mn_5O_{12}}$ composite powders post-treated at 600°C at a constant current density of 23 mA g^{-1} between 2.0 and 4.95 V. Although the $\mathrm{Li_2MnO_3}$ powders had high initial discharge capacity, it showed poor cycle performance. The pure $\mathrm{Li_2MnO_3}$ powders prepared by solid state reaction method had also poor cycle performance [36]. The discharge capacity of the $\mathrm{Li_2MnO_3}$ powders dropped from 258 to 115 after 10 cycles. In contrast, the composite powders with low *x* values below 0.5 showed good cycle performance.

The discharge capacities of the pure $\mathrm{Li_4Mn_5O_{12}}$ and $\mathrm{Li_2MnO_3}\cdot\mathrm{Li_4Mn_5O_{12}}$ composite powders increased slightly during first 3 cycles, and then the capacity monotonically decreased during cycling [11]. The initial discharge capacities of $x\mathrm{Li_2MnO_3}\cdot(1\text{-}x)\mathrm{Li_4Mn_5O_{12}}$ composite powders were 225, 219, and 211 mAh g^{-1} when the x values were 0.5, 0.3, and 0. The discharge capacities of those compounds after 30 cycles were 205, 201, and 183 mAh g^{-1}, respectively. The capacity retentions of the composite powders were 89, 90, and 83 % when the x values were 0.5, 0.3, and 0.

Fig. 7 shows the differential capacity vs. voltage (*dQ/dV*) curves of the $0.5\mathrm{Li_2MnO_3}$-$0.5\mathrm{Li_4Mn_5O_{12}}$ composite powder post-treated at 600°C after various cycles. The oxidation peak near 4.7 V was not observed in the *dQ/dV* curve of the second cycle. Gradual activation of inactive $\mathrm{MnO_2}$ component formed from the $\mathrm{Li_2MnO_3}$ in the first charging process to the active layered $\mathrm{LiMnO_2}$ or spinel $\mathrm{LiMn_2O_4}$ components increased the discharge capacities of the pure $\mathrm{Li_4Mn_5O_{12}}$ and $\mathrm{Li_2MnO_3}\cdot\mathrm{Li_4Mn_5O_{12}}$ composite powders within 3 cycles as shown in Fig. 6. The *dQ/dV* curve of the $0.5\mathrm{Li_2MnO_3}$-$0.5\mathrm{Li_4Mn_5O_{12}}$ composite powders after 30 cycles had the same shape to that of the pure spinel $\mathrm{LiMn_2O_4}$ [33].

4. CONCLUSIONS

The layered-spinel $x\mathrm{Li_2MnO_3}\cdot(1\text{-}x)\mathrm{Li_4Mn_5O_{12}}$ composite cathode powders with various compositions are prepared by spray pyrolysis. The prepared and post-treated $x\mathrm{Li_2MnO_3}\cdot(1\text{-}x)\mathrm{Li_4Mn_5O_{12}}$ powders have aggregated spherical morphologies of the nanometer-sized primary particles irrespective of the compositions of the cathode powders. The initial charge and discharge capacities of $x\mathrm{Li_2MnO_3}\cdot(1\text{-}x)\mathrm{Li_4Mn_5O_{12}}$ powders increase with increasing the amount of $\mathrm{Li_2MnO_3}$ component. Except the $\mathrm{Li_2MnO_3}$, other powders have good cycle performances. It is indicated that although individual $\mathrm{Li_2MnO_3}$ component have poor cycle performance, it can have enhanced the cycling stability of spinel components. The layered-spinel $x\mathrm{Li_2MnO_3}\cdot(1\text{-}x)\mathrm{Li_4Mn_5O_{12}}$ composite cathode powders prepared by spray pyrolysis have high initial discharge capacities and good cycle properties.

ACKNOWLEDGEMENT

This work was supported by the National Research Foundation of Korea(NRF) grant funded by the Korea government(MEST) (No. 2012R1A2A2A02046367). This study was supported by the Converging Research Center Program through the National Research Foundation of Korea (NRF) funded by the Ministry of Education, Science and Technology (2011-50210).

References

1. J.M. Tarascon, W.R. McKinnon, F. Coowar, T.N. Bowmer, G. Amatucci, D. Guyomard, *J. Electrochem. Soc.,* 141 (1994) 1421
2. R.J. Gummow, A. de Kock, M.M. Thackeray, *Solid State ionics,* 69 (1994) 59
3. M.M. Thackeray, M.F. Mansuetto, D.W. Dees, D.R. Visser, *Mater. Res. Bull.*, 31 (1996) 133
4. T. Takada, H. Hayakawa, E. Aklba, *J. Solid State Chem.,* 115 (1995) 420
5. T. Takada, H. Hayakawa, T. Kumagal, E. AkJba, *J. Solid State Chem.,* 121 (1996) 79
6. M.N. Richard, E.W. Fuller, J.R. Dahn, *Solid State lonics,* 73 (1994) 81
7. J.M. Tarascon, D. Guyomard, *Electrochim. Acta,* 38 (1993) 1221
8. C.S. Johnson, *J. Power Sources*, 165 (2007) 559
9. J. Wang, Y. Xia, X. Yao, M. Zhang, Y. Zhang, Z. Liu, *Int. J. Electrochem. Sci.,* 6 (2011) 6670
10. A. Du Pasquier, A. Blyr, P. Courjal, D. Larcher, G. Amatucci, B. Gerand, J.M. Tarascon, *J. Electrochem. Soc.,* 146 (1999) 428
11. C.S. Johnson, N. Li, J.T. Vaughey, S.A. Hackney, M.M. Thackeray, *Electrochem. Commun.,* 7 (2005) 528
12. R. Santhanam, B. Rambabu, *Int. J. Electrochem. Sci.,* 4 (2009) 1770
13. C.S. Johnson, N. Li, C. Lefief, M.M. Thackeray, *Electrochem. Commun.,* 9 (2007) 787.
14. Y. Wu, A. Manthiram, *Electrochem. Solid-State Lett.,* 9 (2006) A221
15. C.S. Johnson, N. Li, C. Lefief, J.T. Vaughey, M.M. Thackeray, *Chem. Mater.,* 20 (2008) 6095
16. C.S. Johnson, J.S. Kim, C. Lefief, N. Li, J.T. Vaughey, M.M. Thackeray, *Electrochem. Commun.,* 6 (2004) 1085
17. F. Wu, H. Lu, Y. Su, N. Li, L. Bao, S. Chen, *J. Appl. Electrochem.,* 40 (2010) 783
18. P.S. Whitfield, S. Niketic, I.J. Davidson, *J. Power Sources,* 146 (2005) 617
19. B.L. Ellis, K.T. Lee, L.F. Nazar, *Chem. Mater.,* 22 (2010) 691
20. J.S. Kim, C.S. Johnson, J.T. Vaughey, M.M. Thackeray, *J. Power Sources,* 153 (2006) 258
21. H. Deng, I. Belharouak, R.E. Cook, H. Wu, Y.K. Sun, K. Amine, *J. Electrochem. Soc.,* 157 (2010) A447
22. T. Ohzuku, M. Nagayama, K. Tsuji, K. Ariyoshi, *J. Mater. Chem.,* 21 (2011) 10179
23. I. Taniguchi, C.K. Lim, D. Song, M. Wakihara, *Solid State Ionics*, 146 (2002) 239
24. S.H. Ju, D.Y. Kim, E.B. Jo, Y.C. Kang, *J. Mater. Sci.,* 42 (2007) 5369
25. I. Taniguchi, N. Fukuda, M. Konarova, *Powder Technology*, 181 (2008) 228
26. S.H. Park, C.S. Yoon, S.G. Kang, H.S. Kim, S.I. Moon, Y.K. Sun, *Electrochim. Acta,* 49 (2004) 557
27. S.H. Ju, H.C. Jang, Y.C. Kang, *Electrochim. Acta,* 52 (2007) 7286
28. Y.N. Ko, H.Y. Koo, J.H. Kim, J.H. Yi, Y.C. Kang, J.H. Lee, *J. Power Sources,* 196 (2011) 6682
29. I. Taniguchi, D. Song, M. Wakihara, *J. Power Sources,* 109 (2002) 333
30. S.H. Park, Y.K. Sun, *Electrochim. Acta,* 50 (2004) 431
31. Y.N. Ko, J.H. Kim, Y.J. Hong, Y.C. Kang, *Mater. Chem. Phys.*, 131 (2011) 292
32. K. Matsuda, I. Taniguchi, *J. Power Sources,* 132 (2004) 156
33. S.H. Park, Y. Sato, J.K. Kim, Y.S. Lee, *Mater. Chem. Phys.*, 102 (2007) 225
34. X.J. Guo, Y.X. Li, M. Zheng, J.M. Zheng, J. Li, Z.L. Gong, Y. Yang, *J. Power Sources,* 184 (2008) 414
35. T. Takada, E. Akiba, F. Izumi, B.C. Chakoumakos, *J. Solid State Chem.*, 130 (1997) 74
36. D.Y.W. Yu, K. Yanagida, Y. Kato, H. Nakamura, *J. Electrochem. Soc.*, 156 (2009) A417
37. T. Takada, H. Hayakawa, E. Akiba, F. Izumi, B.C. Chakoumakos, *J. Power Sources,* 68 (1997) 613
38. Z. Lu, J.R. Dahn, *J. Electrochem. Soc.*, 149 (2002) A815